JOC The Journal of Organic Chemistry

Article

pubs.acs.org/joc

Regioisomerism in the Synthesis of a Chiral Aminotetralin Drug Compound: Unraveling Mechanistic Details and Diastereomer-Specific In-Depth NMR Investigations

Peter Schuisky, Hans-Jürgen Federsel,* and Wei Tian*

Pharmaceutical Development, AstraZeneca, 151 85 Södertälje, Sweden

Supporting Information

ABSTRACT: During chemical process development of a novel 2-aminotetralin derivative intended for use as an antidepressant, scrutiny of the byproduct present in the drug molecule revealed a set of regioisomers. Detailed studies showed that this impurity issue originated from an early synthetic step in which a brominated tetralone motif was generated in a ring-closing protocol. It was found that this reaction was accompanied by a migration of the aromatic bromo substituent via different bromonium species along two discrete pathways. This example of the halogen dance reaction resulted in the formation of a series of tetralone impurities with a bromine distributed across all available aromatic positions of the tetralin nucleus. Subsequently, when subjected to reductive amination conditions, each of these tetralones gave rise to pairs of aminotetralins in a diastereomeric relationship. NMR investigations revealed that the alicyclic portion of the compounds thus formed displayed very complex signal patterns, which required further in-depth studies using a variety of sophisticated techniques. As a result, a deep insight into the structural features of the current 2-aminotetralin family was obtained, which is emphasized by the definition of a novel "0.2 ppm rule" allowing the absolute configuration at tetralin C-2 to be determined.

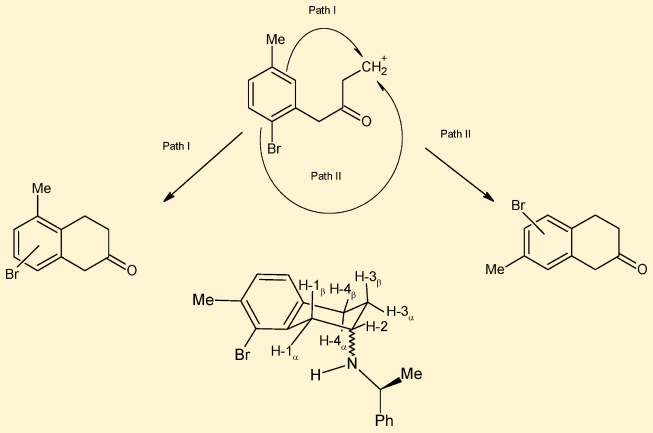

INTRODUCTION

Medicines, for example in the form of tablets, ointments, or injectables, might appear to be relatively simple products far from the high-tech goods that surround our daily life. Nothing could be more wrong as there is indeed a lot of specialized knowledge and sophisticated science that needs to be put in place covering a broad range of investigations and activities including understanding disease mechanisms, design of pharmacologically active molecules, safety assessment, process development and scale up, documentation of clinical efficacy, commercial production, performance testing, and distribution before the final drug can be offered to patients. Every area and discipline involved has its own intrinsic problems and challenges together with an associated arsenal of methodologies defining how to address them. From the viewpoint of an end-user (i.e., a patient), there is obviously a special emphasis on the quality aspects and integrity of a pharmaceutical product that eventually will be dosed with the aim to improve health. In this context, the demands from health authorities and regulatory bodies have become ever more stringent over time, and this development has, to a large extent, proceeded in parallel to the dramatic improvement in analytical sciences and techniques, allowing impurities to be detected in successively smaller and smaller amounts. Thus, finding trace amounts of a broad variety of components, both organic and inorganic, at ppm levels is more or less commonplace with a further expansion to the nano (10^{-9} g) and pico (10^{-12} g) domains and onward already well underway. Hand in hand with this, the capability to determine the structural features of increasingly complex molecular entities has seen an enormous expansion over the past decades, so it is absolutely true to say that whenever foreign materials are present in a sample matrix the likelihood of their detection and structure elucidation is very high.

BACKGROUND

During the course of a development project initiated in the late 1990s targeting a novel agent for the treatment of various illnesses located in the central nervous system (CNS) such as anxiety and depression, we were faced with a highly intriguing problem. This concerned a series of positional isomers (regioisomers) generated along the synthetic pathway with a potential to impact the quality attributes of the final drug molecule, the 5-HT_{1B} antagonist AR-A2 (**1**)[1−3] originating

Received: February 22, 2012
Published: June 4, 2012

   dx.doi.org/10.1021/jo300277y | J. Org. Chem. 2012, 77, 5503−5514

from discovery efforts in former Astra and then progressed by AstraZeneca, in a negative fashion.

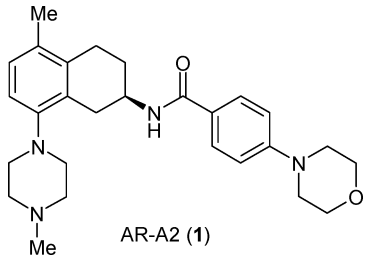

AR-A2 (**1**)

The initial investigations performed on this chiral aminotetralin compound were based on a material that was prepared using a synthetic route devised by the medicinal chemistry team.[4−6] Ruling out this initial synthesis method as impractical for scale up, a new way of making the desired product **1** had to be found. Thus, 3-methylphenylacetic acid (**2a**), commercially available in bulk quantities at an attractive price, was identified as the building block of choice.

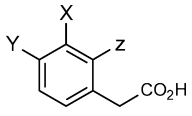

2a-c

2a: X=Me, Y=H, Z=H
b: X=H, Y=H, Z=Me
c: X=H, Y=Me, Z=H

In merely three steps, compound **2a** was nicely converted to an (*R*)-aminotetralin derivative ready for further chemical manipulations (Scheme 1a). Subsequently, the Buchwald−Hartwig protocol offered a smooth attachment of the piperazinyl substituent via displacement of the bromide, and the sequence is finished off by a deprotection immediately followed by introduction of the side-chain carboxylic acid residue in an amide-generating transformation. Further improvements of this second-generation process[5,6] enabled the efficient stereochemical induction in the imine → amine step by using the chiral *N*-donating reagent (*S*)-1-phenylethylamine (Scheme 1b) in contrast to operating in a racemic mode combined with a resolution (Scheme 1a). When applying this third-generation synthesis,[5,6] the overall yield of comparable stages in routes 2 and 3, respectively, starting from **2a** was roughly doubled (10−13% vs 4−6%); a step change crucial to the sustainability of the method and a successful scale up to multikg batch size. In spite of interesting and promising pharmacological properties[7] manifested in early clinical trials (phase I and II) on healthy volunteers and small patient groups, respectively, the project had to be abandoned because of some undesirable side effects when tested in man.

Quality Aspects of the Drug Molecule. As the end product (**1**) thus prepared constituted the active ingredient in the drug under development, the full characterization of the quality attributes was essential to match the stringent regulatory requirements put up by the health authorities to enable further testing in humans. Besides the establishment of "standard"-type analytical data such as chromatographic purity, enantiomeric composition, assay, and confirmation of identity (e.g., by IR) there has to be a strong emphasis on the identification of impurities. Thus, the generally accepted level where byproducts have to be fully identified and their structures verified is ≥0.1%, unless they show or can be suspected to carry pronounced properties of toxicity (as is the case with genotoxic impurities[8]) where the demand is rather in the ppm range. In the present case, when conducting thorough analyses on crude samples of product **1** from laboratory trials, it became apparent that there was a spectrum of organic contaminants present. Careful investigation, albeit not attempting to establish a detailed assay of each component, showed that these constituted a series of five regioisomeric analogues of target compound AR-A2 (**1**), the structures of which were unambiguously identified as **3a−e** (Figure 1).

RESULTS AND DISCUSSION

Synthetic Chemistry. Homing in on the underlying cause for the impurity profile thus observed, our attention was devoted to the very first step in the sequence, which is common to both second- and third-generation routes. In this literature-based method,[9] the aromatic carboxylic acid starting material **2a** was treated with elemental Br_2 (slight excess of 2.5 mol %) in the presence of K_2CO_3 as base under aqueous conditions.[6] After an extractive workup was conducted, the crude product was isolated and the analysis revealed a relative composition (HPLC) of monobromo isomers **4a−c** of 55/34/8 (total yield 30−35%), respectively, besides a minor amount (1%) of the dibrominated species **4d**. Recrystallization in an aqueous/organic medium (H_2O/*i*-PrOH/HOAc) improved the isomer distribution to 80/14/4. Repeating this procedure (H_2O/*i*-PrOH) finally raised the overall purity to 95% with regard to the desired regioisomer **4a**, leaving the other isomeric impurities at 2.5% (**4b**) and 1.5% (**4c**) relative abundance, respectively. The material prepared in this way showed a good correlation with literature data[10] and was then used as is in the following step, which after subsequent transformations, led to the final product in the form of aminotetralin **1**. The evident task was to explain in mechanistic terms how, alongside **1**, a range of positional analogues (**3a−e**) could be formed, inasmuch as the bromination step had rendered only two monobromide contaminants **4b,c** (besides the desired isomer **4a** and trace amounts of the dibromo analogue) as far as our scrutiny could tell.

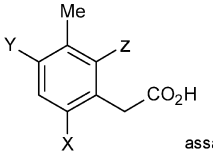

4a-d

	assay after purification (area-% GC)
4a: X=Br, Y=H, Z=H	95
b: X=H, Y=Br, Z=H	2.5
c: X=H, Y=H, Z=Br	1.5
d: X=Br, Y=Br, Z=H	-

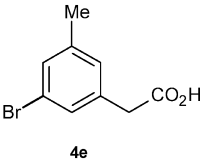

4e

A suitable starting point for our in-depth investigation was to realize that bromo acid **4a** could engage in the subsequent ring-forming step and that it was equally possible for isomers **4b,c**. A search for known facts about the C_2-based method applied for creating the tetralone moiety, a synthesis originally devised in the early 1960s[11] and considered to be one of the most efficient procedures for the formation of this structural motif, eventually directed us to work conducted about a decade later. The particular study[12] showed that *o*-methylphenylacetic acid (**2b**) gives rise to a mixture of two products in a 2:1 ratio, besides demonstrating that a drastically improved overall yield was obtained when switching the solvent from CS_2 to CH_2Cl_2. By comparing these in analytical terms (i.e., by NMR and UV)

dx.doi.org/10.1021/jo300277y | J. Org. Chem. 2012, 77, 5503−5514

Scheme 1. Modified and Optimized Syntheses of AR-A2 (1): (a) Second-Generation Route; (b) Third-Generation Route

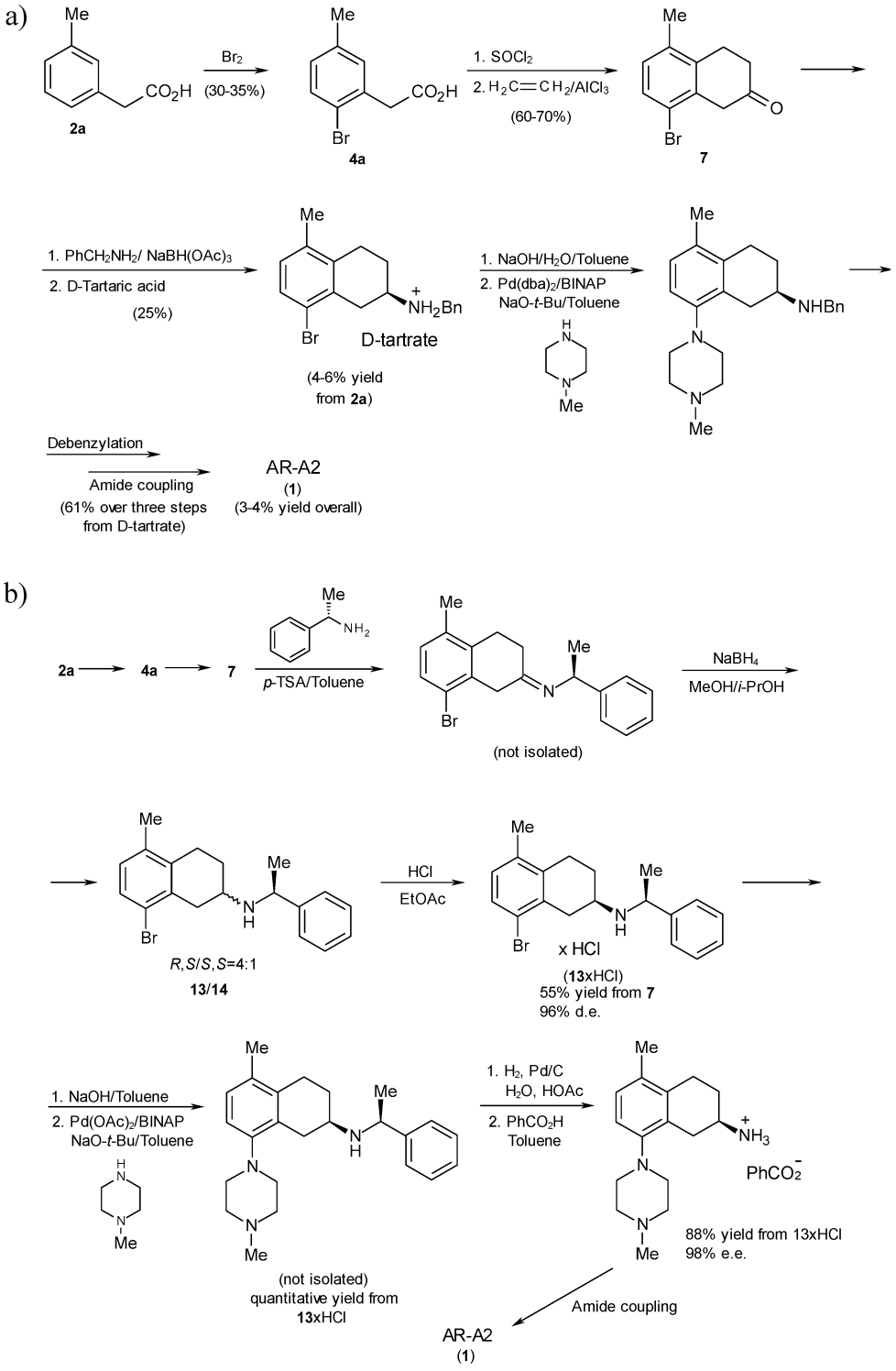

with the compounds generated when subjecting the *meta*- (**2a**) and *para*-isomers (**2c**) to identical reaction conditions [2 (5- and 7-isomers) and 1 (6-isomer) product(s) were formed, respectively], it was unambiguously confirmed that the *ortho*-substituted substrate led to 5-methyl-ß-tetralone (**5**; unexpected) and its 8-congener (**6**; expected) in 2:1 relative amounts (Scheme 2). These findings strongly indicated that in order to explain the formation of **5**, a molecular rearrangement had to take place, and the suggested mechanism was based on the migration of the methyl substituent. Thus, the electrophilic Friedel−Crafts related alkylation was thought to initially create a secondary cation, which by virtue of a 1,2-Me transposition, turned into a tertiary carbonium ion driven by an increase in stability of the latter. A subsequent rearomatization finished the overall sequence off, turning starting material **2b** into tetralone **5** (Scheme 2).

The current case expressed obvious similarities in that the starting material for the ring-formation featured the methyl

dx.doi.org/10.1021/jo300277y | J. Org. Chem. 2012, 77, 5503−5514

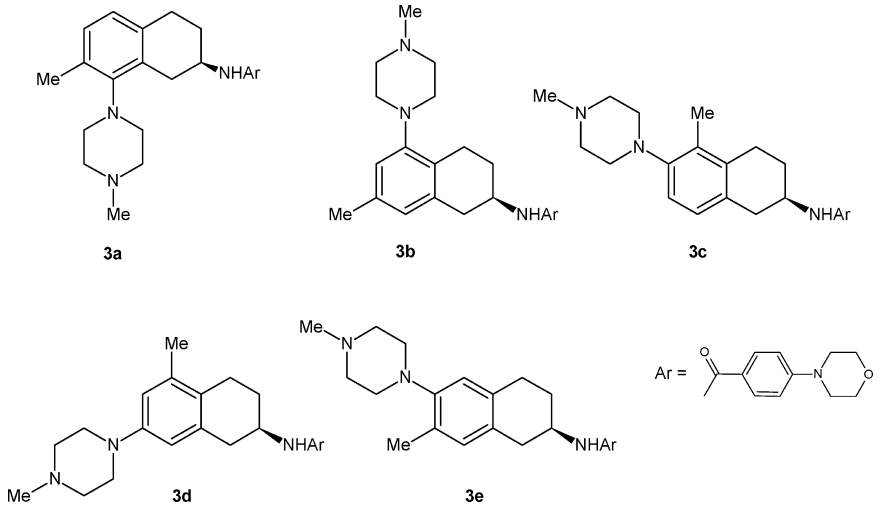

Figure 1. Analogues of AR-A2 (**1**): structures of impurities in regioisomeric relationship to the final product and first identified in laboratory samples.

Scheme 2. Methyl Migration Is Accountable for the Formation of the Unconventional 5-Isomer (5) alongside the Expected 8-Isomer (6) in the Ethene-Based Ring-Closure of 2-Methylphenylacetic Acid under Friedel–Crafts Conditions[12]

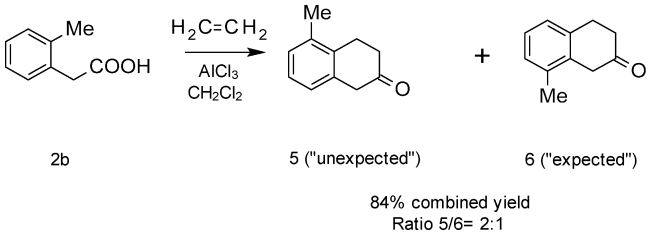

group in a *meta*-position to the carboxylic acid appendage. However, insertion of a Br substituent added extra molecular complexity to the system, which was further enhanced by the fact that the purified material after the bromination step to be used in the subsequent transformation still contained the two nondesired isomers **4b,c** in far from negligible amounts. Our thorough analysis (LC–MS) of the isolated product after the ring closure had been conducted clearly confirmed this as, besides the wanted 8-bromo-5-methyltetralone **7**, a series of five further analogues (**8**–**12**) were identified (Figure 2). Besides the main product **7** appearing in an abundance of 86.8 area % on GC analysis, the impurities (**8**–**12**) were found to be present spanning a content range from 0.24 to 5.96 area % in the crude material (Figure 3).

Interestingly, in all of these byproducts the *meta* relationship between the carboxymethyl and methyl substituents present in the starting material **2a** was kept intact, which by analogy with the literature example described previously, strongly pointed in the direction of a rearrangement mechanism coming to play. In our case, the evidence at hand, however, implied a migration of the Br group as being accountable for the observed results. As a matter of fact, the phenomenon of migrating halogen atoms in aromatic systems (notably belonging to the class of benzene derivatives) had previously been reported in the literature. The original discovery dates back more than 60 years, to the early 1950s,[13] and this peculiar reaction type is known by different

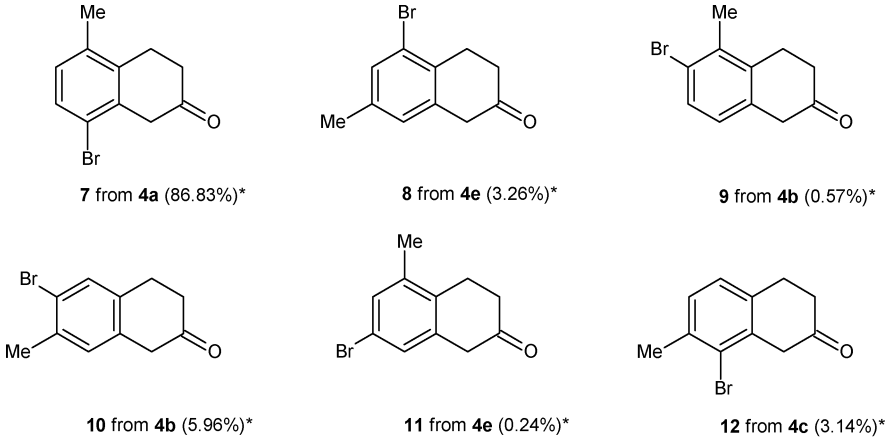

* Abundance found in crude reaction mixture from lab experiment, 3rd generation route

Figure 2. Cluster of bromomethyl-2-tetralones **8**–**12** formed alongside the desired isomer **7** during the ring-closing step of 2-bromo-5-methylphenylacetic acid (**4a**) with ethene as C_2-building block under Friedel–Crafts-like conditions. Absolute verification of the structures of byproduct **8**–**12** was achieved through directed syntheses from bromomethylphenylacetic acid isomers **4b,c,e** (see above) as noted.

dx.doi.org/10.1021/jo300277y | J. Org. Chem. 2012, 77, 5503–5514

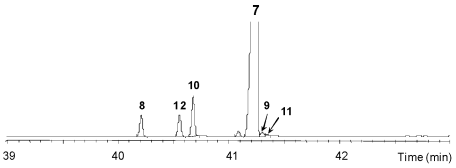

GC chromatogram revealing separation of regioisomers of tetralones from a crude product from actual industrial batch.
GC column: DB-1701, 30 m x 0.25 mm x 0.25 μm; Injection temperature 250°C, carrier gas: Helium, Constant flow 1.5 ml/min; temperature profile: 115°C (30 min), 10°C/min 280°C (10 min).

Figure 3. GC trace showing the mixture of regioisomeric tetralones **7**−**12** as formed during an authentic pilot plant run of the ring-closing reaction between phenylacetic acid **4a** (synthesis quality containing small percentages of **4b**,**c**) and ethene. The numbers on the peaks refer to the tetralone structures **7**−**12** featured in Figure 2.

names such as halogen scrambling, halogen migration, and halogen isomerization, but with halogen dance standing out as the by far most commonly utilized expression, probably by virtue of its illustrative power in describing what is taking place on a molecular level.[14] Thus, by subjecting multiply halogenated benzenes, the "classical" substrate in this context,[15] to the treatment with strong base (for example, alkali amides) a spectrum of products are obtained whose structure and mechanism of formation have been thoroughly investigated. A full understanding of this puzzling transformation was not reached until the early 1970s, and the current view is that a cascade of events composed of deprotonation in the form of a metal−hydrogen exchange coupled with a corresponding metal−halogen exchange most likely are accountable for the experimental data.[14,16] In the present case, however, it is important to emphasize that the observed rearrangement occurred under Lewis acidic conditions ($AlCl_3$). Detailed investigations by the Olah[17] group starting in the early 1960s have shown that depending on the nature of the halogen and alkyl substituents, respectively, either group can undergo migration. Specifically, they found that in the class of bromocumenes there was a mix in the migratory amplitude involving both the halide and alkyl moieties.

The key question for us to address was to shed light on how each of the brominated species **4a**−**c** (which are all present in the synthesis quality material) was transferred into the corresponding product(s). In order to unravel this phenomenon, it was decided to first perform a control experiment where highly purified **4a** (virtually lacking any of the regioisomeric monobromides), the 2-bromo-5-methyl isomer of the starting acid, was subjected to identical reaction conditions as specified in the authentic protocol. Much to our surprise, a careful analytical scrutiny of the isolated material revealed that it did not consist of just a single product as we had anticipated but was composed of a complex mixture of compounds. Thus, unexpectedly, besides predicted tetralone **7**, all the other five previously identified byproduct **8**−**12** (Figure 2) were also present. The only observable difference compared to running the reaction with the authentic, nonpurified material consisting of **4a**−**c** was that the relative amounts of the various tetralones deviated slightly. To eliminate any doubt about the correctness of the suggested structures, all bromomethyl tetralone isomers **7**−**12** that had been generated during the ring-formation were synthesized[18,19] separately (Scheme 3) and shown to be identical to the components in the crude reaction product. In these independent syntheses, each targeted tetralone was the main product but, as expected, the experiments resulted in isomeric mixtures.

Our conclusions from these findings were that the bromo substituent in the substrate displayed promiscuous behavior toward migration under the current conditions that eventually resulted in the occupancy of all available positions on the aromatic ring. A mechanistic model that takes account of the formation of the observed 5-, 6-, 7-, and 8-bromotetralin regioisomers **8**−**12**, respectively, building on the formation of intermediary bromonium ion species, is suggested (Scheme 4). Of these, the tentative mechanism to compound **12** requires a somewhat more delicate migration path for the bromonium ion: From the common intermediate in path II, two possible migration directions are available. The bromo substituent can either migrate along the outer border of the aromatic ring system or across the C−C bond junction (bridge pathway) to unite the two rings. In all likelihood, the latter mechanism is the most plausible one, by virtue of the extra stability gained by the bromonium ion across the bridge in spite of some steric crowding. The outer pathway we find less likely, due to a possible steric hindrance imposed by the Me group.

At this stage, we decided to take the chemistry one step forward. The driver for this was that we wanted to follow the fate of each of the tetralone derivatives following the downstream processing and to unravel whether any of the byproduct formed along the way would eventually be traceable in the final substance. In order to achieve this, proper analyses had to be devised guaranteeing that small impurity amounts (down to a level of 0.1%) could be detected and structurally characterized. As a first step in this direction, it was essential to conduct further studies on the pure compounds in isolation rather than using authentic mixtures generated in the synthetic process. Thus, each of the regioisomeric tetralones (**7**−**12**), prepared according to the sequences outlined in Schemes 1a

Scheme 3. Generic Synthetic Procedure for Preparing Authentic Samples of Regioisomeric Bromomethylphenylacetic Acids 4c,e[a]

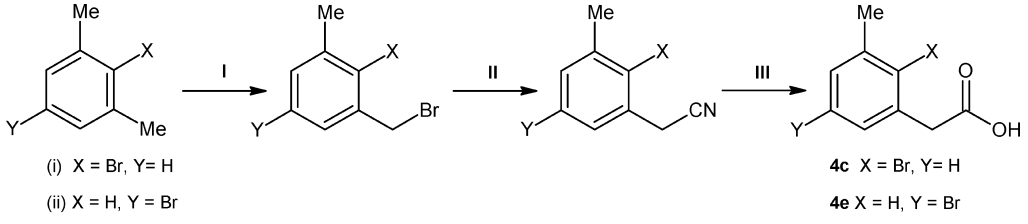

[a]Abbreviations: NBS, *N*-bromosuccinimide; BnOOBn, dibenzoyl peroxide; DCM, dichloromethane.

dx.doi.org/10.1021/jo300277y | *J. Org. Chem.* 2012, 77, 5503−5514

Scheme 4. Mechanistic Model That Accounts for the Formation of 2-Tetralones 7−12 from a Common Carbocation Intermediate Generated under Friedel−Crafts Conditions and Following Either Path I (Leads to 7, 9, and 11) or Path II (Leads to 8, 10, and 12)

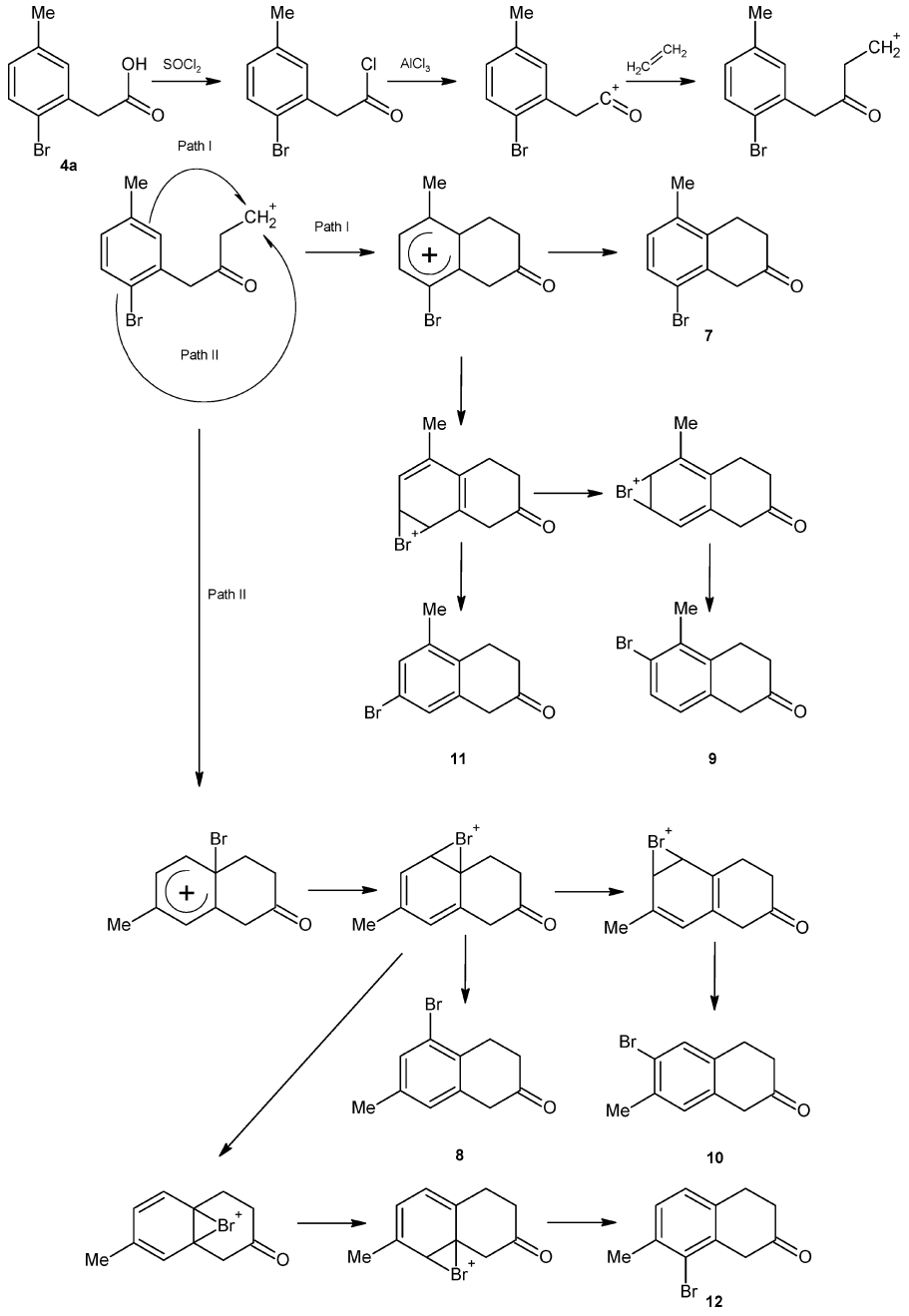

and 3, was subjected to the conditions defined for the reductive amination in the third-generation route (Scheme 1b).[6] In all six cases, this resulted in a pair of diastereomerically related aminotetralins displaying the expected ratio (*R*,*S*)/(*S*,*S*) ≈ 4:1 (Scheme 1b). These two-component mixtures were subsequently separated via chromatography to yield highly enriched samples of all 12 diastereomers **13**−**24** (see Figure 4 and the Experimental Section for details).

A meticulous tracking exercise was conducted to follow the impurities found at the tetralone stage (**8**−**12**) further downstream along the synthetic pathway, to see if and in what form they were carried over to eventually appear as byproduct in later intermediates and the final compound. It turned out that there was no purification in the reductive amination step, and so all tetralones were transformed into the corresponding aminotetralins **13**−**24** (even if primary analysis showed that one of the analogues was missing, which, however, could be corrected as its presence was detected under the main peak after spiking experiments). When the penultimate intermediate (in the form of the benzoate salt; Scheme 1b) was reached, the number of components had not shrunk by more than one, leaving the main product contaminated with four isomeric impurities. Finally, a more efficient up-grading of the quality took place over the last bond-forming step (amide coupling), the subsequent workup, and product precipitation leading to AR-A2 (**1**) containing merely structural isomer **3b**, fortuitously only in trace amounts.

dx.doi.org/10.1021/jo300277y | *J. Org. Chem.* 2012, 77, 5503−5514

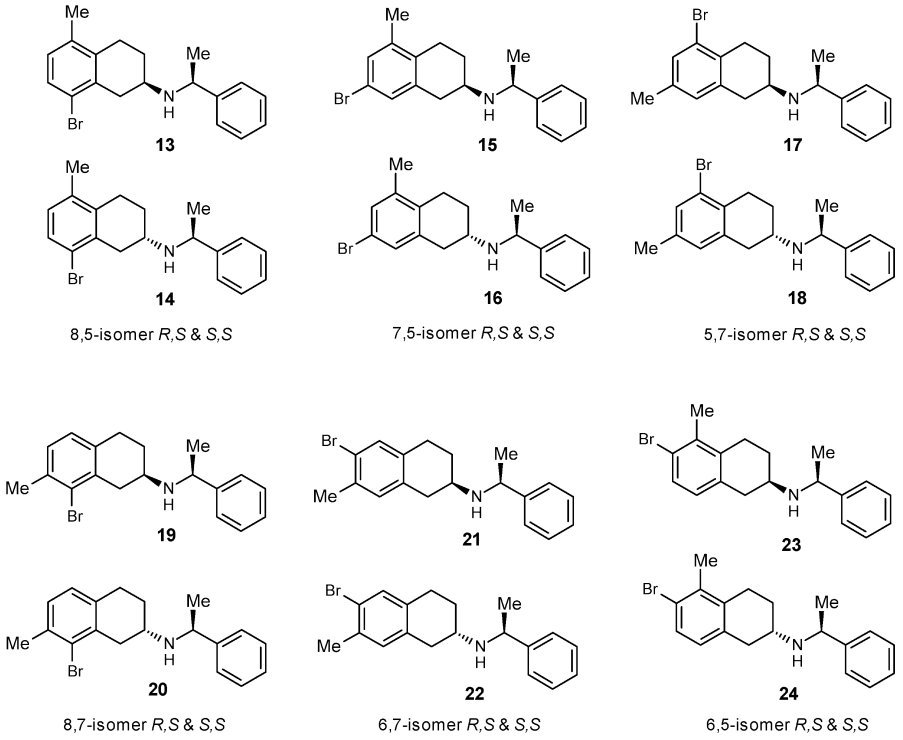

Figure 4. Six pairs of 2-aminotetralin diastereomers **13**/**14**–**23**/**24** formed from 2-tetralones **7**–**12** via the reductive amination step outlined in Scheme 1b.

NMR Investigations. An in-depth NMR study involving both 1D- and 2D-techniques was carried out on the previously mentioned aminotetralin diastereomers **13**–**24** with the aim to unambiguously establish their respective structure. All spectra were recorded on the free base of the compounds, and the focus was primarily the tetralin ring system, as this constituted the part of the molecule where a differentiation between various diastereomers would, most likely, be evident. Hence, the detailed assignment of the signals attributed to the phenyl ring in the phenethyl side chain has been ignored (a full assignment, however, is presented for compound **22** in the Supporting Information).

In 6-membered cyclic systems, the diaxial coupling constants are, normally, significantly larger than either the axial/equatorial or equatorial/equatorial counterparts; typically 8–13 Hz vs 2–6 Hz, respectively. However, in a distorted system that no longer occupies a "perfect" chair conformation, featuring, for example, a tetralin arrangement, these "rules of thumb" break down and cannot be applied any longer. Hence, a system where the cyclohexyl moiety is fused to an aromatic ring and, furthermore, carries an aryl-substituted amine side chain as is the case in compounds **13**–**24**, forces the cyclohexane to assume an almost twisted chairlike structure. As a consequence, this conformational change also causes the coupling constants between ring protons to undergo a drastic shift. Thus, the diaxial coupling constants decrease, whereas the axial/equatorial and equatorial/equatorial counterparts increase. In this twisted conformer, the protons can no longer be properly described as being either axial or equatorial; instead, they should be characterized as hybrids, having a direction in space that is somewhere in-between these extremes. A more suitable terminology would be to name them α- and β-protons, respectively, depending on whether they are below or above the pseudoplane of the ring in full analogy to common practice applied in the carbohydrate field (exemplified by diastereomer **17**; Figure 5). However, following accepted nomenclature

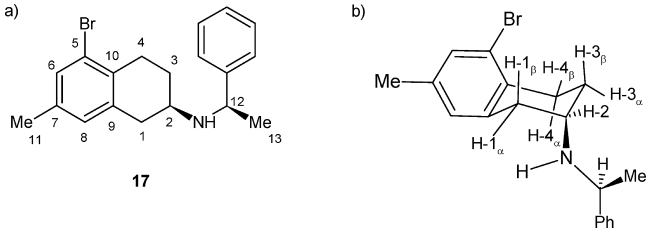

Figure 5. Diastereomer **17** (5,7-isomer in (*R*,*S*) configuration) in (a) a planar presentation and (b) as a three-dimensional framework where the twisted chair has been replaced with a plain chair conformation as a means to enable a clear visibility of crucial protons.

conventions, the use of the axial/equatorial descriptor terminology will be retained when referring to coupling constants. Furthermore, with the aim to convey the spatial arrangements pertaining to the cyclohexane moiety, the 3-D structure is drawn in a chair form which offers a less congested appearance and, therefore, a better clarity.

The starting point for the assignment of ^{1}H NMR signals is proton H-12, attached to the stereogenic carbon atom C-12 located in the side chain appendage of tetralin intermediates **13**–**24**. From this position, H-2 attached to the stereocenter of the tetralin ring can subsequently be assigned. When protons are present at aromatic carbon atoms 5 and 8, respectively, the correlation between these and the protons on the alicyclic portion of the molecule can be used as a further assigning tool. Generally, in the ^{1}H NMR spectra of these diastereomeric tetralins, several of the signals overlap, and for many of the protons the splitting patterns are so complex that all signals coalesce, leading to the recorded signal being very broad.

dx.doi.org/10.1021/jo300277y | J. Org. Chem. 2012, 77, 5503–5514

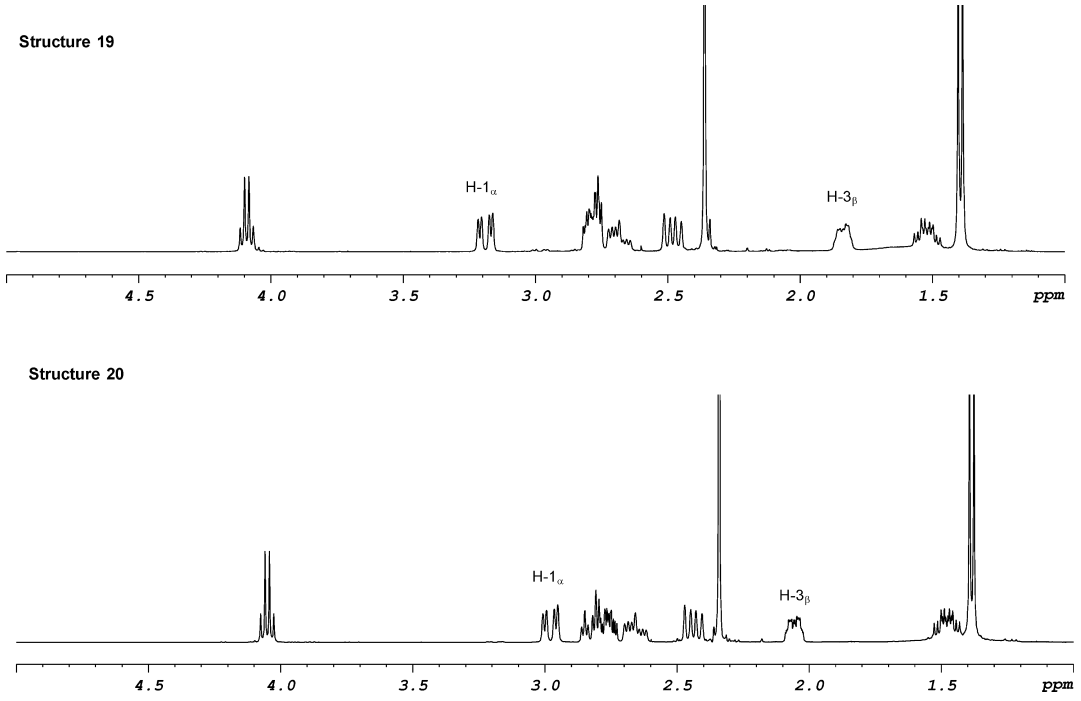

Figure 6. ^{1}H NMR spectra of the separated diastereomeric 8/7-regioisomer pair **19** (*R,S*) and **20** (*S,S*), above and below, respectively, where the ~0.2 ppm shift difference displayed by signals from H-1$_\alpha$ and H-3$_\beta$ are clearly visible.

Table 1. ^{1}H Coupling Constants of Regioisomeric 2-Aminotetralins 13−24 in Pure Diastereomeric Form[a]

	couplings constants (Hz)									
2-aminotetralin diastereomer	$J_{1ax,1eq}$	$J_{1ax,2ax}$	$J_{1eq,2ax}$	$J_{2ax,3ax}$	$J_{2ax,3eq}$	$J_{3ax,4ax}$	$J_{3ax,4eq}$	$J_{3eq,4ax}$	$J_{3eq,4eq}$	$J_{4ax,4eq}$
13 (8,5; *R,S*)	16.7		4.4							
14 (8,5; *S,S*)										
15 (7,5; *R,S*)						10.7	6.0			17.6
16 (7,5; *S,S*)						10.6	5.3			17.8
17 (5,7; *R,S*)	16.0		3.7			10.4	5.1			17.7
18 (5,7; *S,S*)						10.4	5.1			17.7
19 (8,7; *R,S*)	16.9	9.0	5.2			10.8	5.4			16.2
20 (8,7; *S,S*)	17.0	7.8	4.6						4.8	16.7
21 (6,7; *R,S*)	16.1	8.9	4.7			10.8		6.0		16.8
22 (6,7; *S,S*)	17.2	10.4				10.9		6.3		17.2
23 (6,5; *R,S*)	16.0		3.8			9.4				17.2
24 (6,5; *S,S*)										

[a]Blank space indicates that no clean signal could be recorded.

Table 2. Chemical Shift Values (δ) in the Alicyclic Region of 2-Aminotetralin Diastereomer Pairs 13/14−23/24[a]

	tetralin											
alicyclic proton	**13** (*R,S*)	**14** (*S,S*)	**15** (*R,S*)	**16** (*S,S*)	**17** (*R,S*)	**18** (*S,S*)	**19** (*R,S*)	**20** (*S,S*)	**21** (*R,S*)	**22** (*S,S*)	**23** (*R,S*)	**24** (*S,S*)
H-1$_\beta$	2.40	2.36	2.61	2.52	2.61	2.62	2.48	2.48	2.48	2.44	2.57	2.48
H-1$_\alpha$	**3.07**	**2.86**	**2.98**	**2.77**	**3.03**	**2.80**	**3.19**	**2.99**	**2.93**	**2.74**	**2.97**	**2.72**
H-3$_\beta$	**1.84**	**2.05**	**1.90**	**2.11**	**1.95**	**2.16**	**1.84**	**2.07**	**1.84**	**2.05**	**1.90**	**2.08**
H-3$_\alpha$	1.47	1.44	1.58	1.56	1.63	1.62	1.52	1.49	1.54	1.51	1.58	1.54

[a]The ~0.2 ppm shift difference recorded for H-1α and H-3ß, respectively, within each diastereomeric pair is shown in bold.

Incidentally, only in the 8,7-*R,S*/*S,S* isomer pair **19**/**20** are all protons fully separated (Figure 6).

When the proton signals coalesce in the 1D-spectrum, however, detailed shift values can be obtained by conducting inverse detection experiments such as HMBC and HMQC, and by using this technique on the current array of tetralins (**13**−**24**), the different protons have been assigned to specific carbon atoms. Furthermore, in combination with a series of HMBC studies also the relative positions of all protons have been established, and thus, the whole C−H skeleton has been populated accordingly (^{1}H and ^{13}C NMR data specified in the Experimental Section). In all cases except for one of the pairs, the 6,5-*R,S*/*S,S* isomers **23**/**24**, at least one signal of the C-1 and C-4 protons gave information about the coupling

dx.doi.org/10.1021/jo300277y | J. Org. Chem. 2012, 77, 5503−5514

constants. Therefore, the assignment in the 6,5 case was based entirely on the trend defined by the other tetralins. For the remaining isomers, however, enough information (i.e., coupling constants) was revealed to identify some of the $J_{ax,ax}$ and/or $J_{ax,eq}$ relationships (Table 1).

As mentioned previously, there was an expectation that $J_{ax,ax}$ couplings would have larger numerical values than for $J_{ax,eq}$ even in the current class of distorted systems. Hence, on the basis of this assumption, a tentative assignment for the compound series **13**−**24** was performed (Table 2).

Our interpretation of the large geminal couplings in the range of 16−18 Hz for $J_{1ax,\ 1eq}$ and $J_{4ax,\ 4eq}$, respectively (Table 1), is that they are caused by a decrease in the H−C−H bond angle due to the distorted ring conformation (twisted chair). Because of the complexity of overlapping signals in the alicyclic region of these structures, it is impossible to obtain all spectroscopic data in order to fill the remaining blanks in this table. As the C-3 protons are too split-up to allow determination of any coupling constants, we had to turn to theoretical assumptions. Looking hypothetically on the structural features, it can be expected for a given *R*,*S*/*S*,*S* pair **13**/**14**, **15**/**16**, **17**/**18** etc. to display varying numbers of couplings constants. Therefore, it seems reasonable that a proton equipped with three coupling constants of similar size would be expected to appear in a coalescence mode.

In the twisted-chair conformation assumed by the tetralin system, the ethylphenylamine side chain is flexible enough to be capable of folding to a position either above or below the plane of the ring, depending on whether the configuration is *R*,*S* or *S*,*S* (Figure 7).

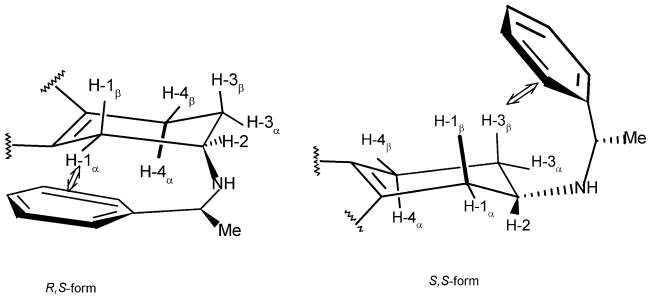

Figure 7. Stereoviews of an unspecified diastereomer pair belonging to the series **13**/**14**−**23**/**24**, where the most plausible twisted-chair conformation has been replaced by a corresponding chairlike setup to better reflect spacious relationships (cf. Figure 5). The difference in orientation of the phenyl ring forming part of the C-2 substituent, above or below the pseudoplane of the tetralin framework, is clearly visible. This, in turn, creates differences in the shielding environment experienced by the protons on the alicyclic portion of the molecule, dependent on whether they assume α or β positions relative to the tetralin ring.

This type of a sandwich-like conformer can be corroborated by conducting "through-space" interaction experiments using NMR and measurements of NOE interactions. Thus, a series of NOESY spectra were recorded where NOE interactions between ring protons on the inner side of the sandwich and the phenyl moiety attached to the C-2 position were measured. In all cases, correlation peaks appear between one of the two C-1 and C-4 protons and the phenyl appendage, whereas the two other appear unaffected. For the C-3 protons no correlation is detected in the experiments, which can be rationalized by the relative location of the phenyl group pointing away from this position in the sandwich arrangement. The strong distance dependence of the NOE effect, the decrease is in inverse proportion to the sixth power of the distance, clearly underpins the statement above that the *S*,*S*-form folds only into a "semi-sandwich" conformation. On the basis of these findings and coupled with theoretical considerations, a full assignment for the entire compound series **13**−**24** has been achieved.

There is, however, an additional effect seen for the C-1 and C-3 protons depending on the actual conformation. Thus, in the 8,7-regioisomers **19**/**20** one of the C-1 protons (H-1$_\alpha$) in the *S*,*S*-stereoisomer **20** appears at a more upfield chemical shift (+∼0.2 ppm) compared to its *R*,*S*-counterpart (Table 2). This rather large difference could possibly be explained by the closeness of the proton in question to the ring current of the adjacent phenyl substituent (Figure 7). Likewise, in the *R*,*S*-form one of the C-3 protons (H-3$_\beta$) shows the same behavior (albeit the shift is downfield going from **19** to **20**) with regard to the chemical shift (+∼0.2 ppm). The feature of a ∼0.2 ppm downfield shift change for one of the H-1 or H-3 protons, respectively, in the *S*,*S* or *R*,*S*-forms in the vicinity of the phenyl group is consistent throughout all six pairs of diastereomers (Table 2). As the aromatic ring current effect does not display the pronounced distance dependence characteristic of NOE, the upfield change of the chemical shift for these protons is a strong indication for the proposed sandwich-like conformers featuring in Figure 7. Therefore, it seems perfectly plausible that the ring current generated by the phenyl moiety is responsible for the effect thus observed.

For the 2-tretralin series **13**−**24** scrutinized, the H-3$_\beta$ proton in the *R*,*S* family appears at 1.8−2.0 ppm whereas in the *S*,*S*-form H-1$_\alpha$ is found in the range 2.7−3.0 ppm. Comparing the shift values between the *R*,*S*- and *S*,*S*-diastereomers for these protons throughout the series of the six tetralin pairs, one finds that the difference always mounts to about 0.2 ppm (±0.02 ppm); e.g., H-1$_\alpha$ at 3.07 in **13** vs 2.86 in **14** and H-3$_\beta$ at 1.84 in **13** and 2.05 in **14**. The predictive power of the relationship thus established has been confirmed via analysis of some analogous 2-aminotetralins, which, thus, validates that the predictions of absolute configuration can be made with a good reliability. This can, however, only be stated as long as the structural features of the compounds scrutinized are reasonably similar to the molecules investigated in this study.

CONCLUSIONS

A close investigation into the causes behind some impurities present in the end product and constituting structural analogues of the chiral 2-aminotetralin drug molecule AR-A2 under clinical development led back to one of the earlier stages in the synthetic pathway. By conducting mechanistic studies, it was possible to confirm that a halogen dance type of reaction was taking place during an $AlCl_3$-mediated ring closure, affording the substituted 2-tetralone motif. Further scrutiny of the spectrum of byproduct thus created and their destiny during the downstream processing, especially applying various advanced NMR techniques which inter alia gave rise to the "0.2 ppm rule", a tool for predicting absolute stereochemistry at the C-2 position of *N*-substituted-2-aminotetralins, has brought about a deeper insight into these molecular systems frequently encountered in the field of medicinal and natural products chemistry. As a consequence of the decision to prematurely discontinue the drug development project of which this study was a part, there was never an opportunity to launch process

dx.doi.org/10.1021/jo300277y | J. Org. Chem. 2012, 77, 5503−5514

modifications with the intention to mitigate or entirely prevent the halogen dance transformation to take place.

EXPERIMENTAL SECTION

NMR spectra were recorded at 298 K on either 500 or 600 MHz spectrometers, when appropriate, equipped with BBI, PABBI, or QNP probes, all of 5 mm dimension. Chemical shift values are listed in parts per million (ppm) downfield from TMS. Coupling constants (J) are given in hertz. The structures were assigned by aid of the following techniques: ^{1}H NMR, ^{13}C NMR, COSY, HMQC, HMBC, NOESY, and ROESY.

General Procedure: Bromination of Bromoxylenes.[18,19] A mixture of 5-bromo-*m*-xylene 25.08 g, (135 mmol), benzoyl peroxide 1.63 g (0.5 mmol), and *N*-bromosuccinimide 29.33 g (163 mmol) was dissolved in dichloromethane (200 mL). A yellow suspension was formed. The mixture was heated to reflux until full conversion was obtained (monitored by GC). The reaction mixture was quenched by addition of a sodium thiosulfate solution (150 mL). The phases were separated and the organic phase removed. The residue was purified by silica chromatography (isooctane) to give 18.6 g (52%) of product.

General Procedure: Cyanation of Bromomethylbenzyl Bromides.[18] To a solution of 3-bromo-5-methylbenzyl bromide 10.89 g (41.3 mmol) in EtOH (160 mL) and H_2O (18 mL) was charged sodium cyanide 2.21 g (45.1 mmol). The mixture was heated at reflux until full conversion (monitored by GC) was reached. The solvent was removed and the crude product extracted with CH_2Cl_2 (100 mL) and H_2O (80 mL). The phases were separated, and the organic phase was removed to give 7.96 g (92%) of product. No further purification was needed.

General Procedure: Hydrolysis to Bromomethylphenylacetic Acids (4c,e).[18] 2-(3-Bromo-5-methylphenyl)acetonitrile (14.78 g, 70.3 mmol) was dissolved in H_2SO_4 (200 mL, 8.6 M) and heated to 140 °C overnight. After cooling, the reaction mixture was extracted with CH_2Cl_2 (100 mL). The solvent was removed. The crude product was mixed with H_2O, and NaOH (aq) was added until a clear solution was formed. The salt solution was extracted with CH_2Cl_2. The H_2O phase was then acidified with diluted HCl allowing the insoluble free acid to precipitate. The reaction gave 13.51 g (84%) of product.

General Procedure: Ring Formation of Tetralones.[6] 3-Bromo-5-methylphenylacetic acid (**4e**) 13.51 g (62.8 mmol) was dissolved in CH_2Cl_2 (50 mL) at room temperature. The solution was heated to 30 °C. Maintaining the elevated temperature, thionyl chloride (18.3 mL, 251 mmol) was added. The mixture was stirred at reflux until complete conversion. At full conversion, excess oxalyl chloride and the solvent were removed. Fresh CH_2Cl_2 (50 mL) was charged to the cold (0 °C) acid chloride solution. The acid chloride solution was then slowly charged to a premade mixture of $AlCl_3$ (9.3 g, 69.1 mmol) and CH_2Cl_2 (60 mL) at 0 °C. The mixture was stirred at 0 °C for 30 min, after which ethene (g) was bubbled into the mixture under stirring. At full conversion (GC), the ethene flow was stopped and the reaction quenched by addition of H_2O. The organic phase was washed with, $NaHCO_3$ (aq), brine, and H_2O. The phases were separated, and the organic phase was removed to give 9.72 g of product in a 4:6 ratio of 5,7- (**8**) and 7,5-tetralone (**11**). The isolated mixture of compounds **8** and **11** was not subjected to any separation attempts, and instead the the reaction progressed in an as-is state in the next step (when attempting isolation in laboratory sale, we noticed a rapid degradation when subjecting the crude product to preparative chromatography).

The selective syntheses of the series of bromomethyl-2-tetralones were conducted from the following starting materials: **8** and **11** from 1-bromo-3,5-dimethylbenzene; **9** and **10** from 4-bromo-3-methylphenylacetic acid; **12** from 2-bromo-1,3-dimethylbenzene.

General Procedure: Aminotetralins 13−24.[6] To a solution containing a mixture of 5,7- and 7,5-tetralone (10.46 g, 43.7 mmol) in toluene (60 mL) were charged *p*-toluenesulfonic acid (0.04 g, 0.22 mmol) and (*S*)-ethylphenylamine (6.05 mL 48.1 mmol). The mixture was heated to 50 °C. After 1 h, the solvent was removed and replaced with MeOH (40 mL). The imine solution was slowly charged to a premade mixture of $NaBH_4$ (2.89 g, 70 mmol) in 2-propanol (60 mL) at 0 °C. Full conversion was obtained after 1 h (GC). The solvents were removed, and the crude product was extracted with a toluene−H_2O (100 mL/100 mL) blend. The organic phase was collected and removed and then replaced by EtOAc (70 mL). To the solution was then charged HCl (6 M) in 2-propanol (20 mL). The crystals formed were filtered off to give 3.65 g (22%). The diastereomeric pairs **15**/**16** and **17**/**18** were separated by preparative LC.

Purification of tetralins **13**−**24** was done on a Chiralpak AD column, 10 μ 20 × 250 mm, using a mixture of 2-propanol/*n*-heptane 4:96 V/V + 0.1% diethylamine as mobile phase.

Analytical data: HRMS were recorded using ESI positive ionization mode[20] calcd for $C_{19}H_{23}BrN$ (M + H) 344.1014.

13: ^{1}H NMR (600 MHz, $CDCl_3$) δ = 1.31 (d J = 6.6 Hz, 3H, H-13), 1.47 (m, 1H, H-3$_\beta$), 1.70 (br 1H, NH), 1.84 (m, 1H, H-3$_\alpha$), 2.04 (s, 3H, H-11), 2.40 (dd J^1 = 16.9 Hz, J^2 = 7.4, 2H, H-1$_\alpha$, H-4$_\alpha$), 2.66 (m, 2H, H-2, H-4$_\beta$), 3.07 (dd J^1 = 16.7 Hz, J^2 = 4.4, 1H, H-1$_\beta$), 4.00 (q, J = 6.6 Hz, 1H, H-12), 6.74 (d, J = 7.8 Hz, 1H, H-6), 7.20 (d, J = 7.8 Hz, 1H, H-7), 7.26−7.37 (m, 5H, Ph-ring) ppm; ^{13}C NMR (100 MHz, $CDCl_3$) δ = 19.4 (C-11), 24.9 (C-13), 26.5 (C-4), 30.0 (C-3), 37.6 (C-1), 50.4 (C-2), 55.1 (C-12), 123.4 (C-8), 128.5 (C-6), 129.5 (C-7), 134.5 (C-5), 135.5 (C-9), 137.5 (C-10), 126.5, 127.0, 128.5, 145.4 (Ph-ring) ppm; HRMS data were recorded using ESI positive ionization mode calcd for $C_{19}H_{23}BrN$ 344.1014, m/z M + 1, 344.1018.

14: ^{1}H NMR (600 MHz, $CDCl_3$) δ = 1.30 (br 1H, NH), 1.31 (d J = 6.6 Hz, 3H, H-13), 1.44 (m, 1H, H-3$_\beta$), 2.05 (m, 1H, H-3$_\alpha$), 2.05 (s, 3H, H-11), 2.36 (m, 2H, H-1$_\alpha$, H-4$_\alpha$), 2.67 (m, 2H, H-2, H-4$_\beta$), 2.86 (m, 1H, H-1$_\beta$), 3.98 (q J = 6.6 Hz, 1H, H-12), 6.74 (d J = 8.1 Hz, 1H, H-6), 7.18 (d J = 8.1 Hz, 1H, H-7), 7.26−7.37 (m, 5H, Ph-ring) ppm; ^{13}C NMR (100 MHz, $CDCl_3$) δ = 19.4 (C-11), 24.9 (C-13), 26.3 (C-4), 28.3 (C-3), 37.6 (C-1), 50.2 (C-2), 54.8 (C-12), 123.1 (C-8), 128.5 (C-6), 129.5 (C-7), 134.8 (C-9), 135.4 (C-5), 137.5 (C-10), 126.5, 126.9, 128.5, 145.9 (Ph-ring) ppm; HRMS data were recorded using ESI positive ionization mode calcd for $C_{19}H_{23}BrN$ 344.1014; m/z M + 1, 344.1018.

15: ^{1}H NMR (600 MHz, $CDCl_3$) δ = 1.36 (d J = 6.6 Hz, 3H, H-13), 1.58 (m, 1H, H-3$_\beta$), 1.80 (br 1H, NH), 1.92 (m, 1H, H-3$_\alpha$), 2.12 (s, 3H, H-11), 2.42 (ddd J^1 = 17.6 Hz, J^2 = 10.7, J^3 = 6.6 Hz, 1H, H-4$_\alpha$), 2.61 (m, 2H, H-1$_\alpha$, H-4$_\beta$), 2.74 (m, 1H, H-2), 2.98 (m, 1H, H-1$_\beta$), 3.98 (q J = 6.6 Hz, 1H, H-12), 7.31 (s, 1H, H-8), 7.08 (s, 1H, H-6), 7.26−7.37 (m, 5H, Ph-ring) ppm; ^{13}C NMR (100 MHz, $CDCl_3$) δ = 19.3 (C-11), 25.0 (C-13), 25.3 (C-4), 30.3 (C-3), 37.6 (C-1), 49.8 (C-2), 55.0 (C-12), 118.8 (C-7), 129.8 (C-8), 130.0 (C-6), 133.7 (C-10), 137.5 (C-9), 138.5 (C-5), 126.5, 127.0, 128.5, 145.4 (Ph-ring) ppm; HRMS data were recorded using ESI positive ionization mode calcd for $C_{19}H_{23}BrN$ 344.1014; m/z M + 1, 344.1015.

16: ^{1}H NMR (600 MHz, $CDCl_3$) δ = 1.36 (d J = 6.6 Hz, 3H, H-13), 1.56 (m, 1H, H-3$_\beta$), 1.80 (br 1H, NH), 2.11 (m, 1H, H-3$_\alpha$), 2.13 (s, 3H, H-11), 2.42 (m, 1H, H-4$_\alpha$), 2.52 (m, 1H, H-1$_\alpha$), 2.68 (dt J^1=17.8 Hz, J^2=10.6, J^3=5.3 Hz, 1H, H-4$_\beta$), 2.75 (m, 1H, H-2), 2.77 (m, 1H, H-1$_\beta$), 4.01 (q J = 6.6 Hz, 1H, H-12), 7.00 (s, 1H, H-8), 7.08 (s, 1H, H-6), 7.26 − 7.37 (m, 5H, Ph-ring) ppm; ^{13}C NMR (100 MHz, $CDCl_3$) δ = 19.3 (C-11), 25.2 (C-13), 28.7 (C-4), 30.1 (C-3), 37.2 (C-1), 49.8 (C-2), 54.9 (C-12), 118.8 (C-7), 129.6 (C-8), 129.9 (C-6), 133.7 (C-10), 137.7 (C-9), 138.5 (C-5), 126.5, 126.9, 128.5, 145.8 (Ph-ring) ppm; HRMS data were recorded using ESI positive ionization mode calcd for $C_{19}H_{23}BrN$ 344.1014, m/z M+1, 344.1015.

17: ^{1}H NMR (600 MHz, $CDCl_3$) δ = 1.44 (d J = 6.6 Hz, 3H, H-13), 1.50 (br 1H, NH), 1.63 (m, 1H, H-3$_\beta$), 1.98 (m, 1H, H-3$_\alpha$), 2.26 (s, 3H, H-11), 2.61 (m, 1H, H-1$_\alpha$), 2.63 (m, 1H, H-4$_\beta$), 2.80 (m, 1H, H-2), 2.89 (dt J^1 = 17.7 Hz, J^2 = 10.4, J^3 = 5.1 Hz, 1H, H-4 $_\alpha$), 3.03 (dd J^1 = 16.0 Hz, J^2 = 3.7 Hz, 1H, H-1$_\beta$), 4.05 (q J = 6.6 Hz, 1H, H-12), 6.85 (s, 1H, H-8), 7.21 (s, 1H, H-6), 7.26−7.37 (m, 5H, Ph-ring) ppm; ^{13}C NMR (100 MHz, $CDCl_3$) δ=19.3 (C-11), 25.0 (C-13), 28.7 (C-4), 30.6 (C-3), 36.8 (C-1), 50.0 (C-2), 55.0 (C-12), 136.7 (C-7), 129.8 (C-6), 130.0 (C-8), 133.7 (C-10), 137.5 (C-9), 138.5 (C-5), 126.5, 127.0, 128.5, 145.4 (Ph-ring) ppm; HRMS data were recorded using ESI positive ionization mode calcd for $C_{19}H_{23}BrN$ 344.1014; m/z M + 1, 344.1011.

dx.doi.org/10.1021/jo300277y | J. Org. Chem. 2012, 77, 5503−5514

18: ^{1}H NMR (600 MHz, $CDCl_3$) δ = 1.40 (br 1H, NH), 1.42 (d J = 6.6 Hz, 3H, H-13), 1.62 (m, 1H, H-3$_\beta$), 2.16 (m, 1H, H-3$_\alpha$), 2.24 (s, 3H, H-11), 2.59 (m, 1H, H-4$_\beta$), 2.62 (m, 1H, H-1$_\alpha$), 2.79 (m, 1H, H-2), 2.80 (m, 1H, H-1$_\beta$), 2.92 (dt J^1 = 17.7 Hz, J^2 = 10.4, J^3 = 5.1 Hz, 1H, H-4$_\alpha$), 4.05 (q J = 6.6 Hz, 1H, H-12), 6.78 (s, 1H, H-8), 7.21 (s, 1H, H-6), 7.26−7.37 (m, 5H, Ph-ring) ppm; ^{13}C NMR (100 MHz, $CDCl_3$) δ = 20.5 (C-11), 24.9 (C-13), 28.6 (C-4), 28.9 (C-3), 37.9 (C-1), 50.0 (C-2), 55.0 (C-12), 136.7 (C-7), 130.6 (C-6), 129.3 (C-8), 132.5 (C-10), 137.4 (C-9), 138.5 (C-5), 126.5, 126.9, 128.5, 145.8 (Ph-ring) ppm; HRMS data were recorded using ESI positive ionization mode calcd for $C_{19}H_{23}BrN$ 344.1014; m/z M + 1, 344.1013.

19: ^{1}H NMR (400 MHz, $CDCl_3$) δ = 1.39 (d J = 6.6 Hz, 3H, H-13), 1.40 (br 1H, NH),1.52 (m, 1H, H-3$_\beta$), 1.84 (m, 1H, H-3$_\alpha$), 2.36 (s, 3H, H-11), 2.48 (dd J^1 = 17.0 Hz, J^2 = 9.0 Hz, 1H, H-1$_\alpha$), 2.69 (ddd J^1 = 16.2 Hz, J^2 = 10.8 Hz, J^3 = 5.4 Hz, 1H, H-4$_\alpha$), 2.75 (m, 2H, H-2, H-4$_\beta$), 3.19 (dd J^1 = 16.9 Hz, J^2 = 5.2 Hz, 1H, H-1$_\beta$), 4.08 (q J = 6.6 Hz, 1H, H-12), 6.89 (d J = 6.6 Hz, 1H, H-5), 6.97 (d J = 6.6 Hz, 1H, H-6), 7.26−7.37 (m, 5H, Ph-ring) ppm; ^{13}C NMR (100 MHz, $CDCl_3$) δ = 23.6 (C-11), 24.9 (C-13), 28.5 (C-4), 29.9 (C-3), 38.0 (C-1), 51.0 (C-2), 55.1 (C-12), 127.3 (C-5), 127.8 (C-6), 128.2 (C-8), 128.5 (C-7), 135.5 (C-10), 136.1 (C-9), 126.5, 127.0, 128.5, 145.4 (Ph-ring) ppm; HRMS data were recorded using ESI positive ionization mode calcd for $C_{19}H_{23}BrN$ 344.1014; m/z M + 1, 344.1016.

20: ^{1}H NMR (400 MHz, $CDCl_3$) δ = 1.40 (d J = 6.0 Hz, 3H, H-13), 1.40 (br 1H, NH),1.49 (m, 1H, H-3$_\beta$), 2.07 (m, 1H, H-3$_\alpha$), 2.34 (s, 1H, H-11), 2.45 (dd J^1 = 16.6 Hz, J^2 = 7.8 Hz, 1H, H-1$_\alpha$), 2.67 (m, 1H, H-4 $_\alpha$), 2.77 (m, 1H, H-2), 2.84 (dt J^1 = 16.7 Hz, J^2 = 4.8 Hz, 1H, H-4$_\beta$), 2.99 (dd J^1 = 17.0 Hz, J^2 = 4.6 Hz, 1H, H-1$_\beta$), 4.06 (q J = 6.5 Hz, 1H, H-12), 6.89 (d J = 7.7 Hz, 1H, H-5), 6.96 (d J = 7.7 Hz, 1H, H-6), 7.26−7.37 (m, 5H, Ph-ring) ppm; ^{13}C NMR (100 MHz, $CDCl_3$) δ = 23.6 (C-11), 25.0 (C-13), 28.2 (C-3), 28.4 (C-4), 39.1 (C-1), 50.8 (C-2), 54.8 (C-12), 127.2 (C-5), 127.8 (C-6), 128.2 (C-8), 135.5 (C-7), 136.0 (C-10), 136.9 (C-9), 126.5, 127.0, 128.5, 145.4 (Ph-ring) ppm; HRMS data were recorded using ESI positive ionization mode calcd for $C_{19}H_{23}BrN$ 344.1014; m/z M + 1, 344.1017.

21: ^{1}H NMR (600 MHz, $CDCl_3$) δ = 1.36 (d J = 6.6 Hz, 3H, H-13), 1.40 (br 1H, NH), 1.54 (m, 1H, H-3$_\beta$), 1.84 (m, 1H, H-3$_\alpha$), 2.29 (s, 3H, H-11), 2.48 (dd J^1 = 16.1 Hz, J^2 = 8.9 Hz, 1H, H-1$_\alpha$), 2.64 (ddd J^1 = 16.8 Hz, J^2 = 10.8 Hz, J^3 = 6.0 Hz, 1H, H-4$_\alpha$), 2.74 (m, 2H, H-2, H-4$_\beta$), 2.93 (dd J^1 = 16.1 Hz, J^2 = 4.7 Hz, 1H, H-1$_\beta$), 4.00 (q J = 6.6 Hz, 1H, H-12), 6.91 (s, 1H, H-8), 7.19 (s, 1H, H-5), 7.26−7.37 (m, 5H, Ph-ring) ppm; ^{13}C NMR (100 MHz, $CDCl_3$) δ = 22.3 (C-11), 25.0 (C-13), 27.3 (C-4), 30.2 (C-3), 35.9 (C-1), 50.3 (C-2), 54.9 (C-12), 121.7 (C-6), 128.5 (C-7), 131.5 (C-8), 132.0 (C-5), 134.7 (C-9), 135.7 (C-10), 126.5, 127.0, 128.5, 145.4 (Ph-ring) ppm; HRMS data were recorded using ESI positive ionization mode calcd for $C_{19}H_{23}BrN$ 344.1014; m/z M + 1, 344.1015

22: ^{1}H NMR (600 MHz, $CDCl_3$) δ = 1.36 (d J = 6.6 Hz, 3H, H-13), 1.40 (br 1H, NH), 1.51 (m, 1H, H-3$_\beta$), 2.05 (m, 1H, H-3$_\alpha$), 2.28 (s, 3H, H-11), 2.44 (dd J^1 = 17.2 Hz, J^2 = 10.4 Hz, 1H, H-1$_\alpha$), 2.64 (ddd J^1 = 17.2 Hz, J^2 = 10.9, J^3 = 6.3 Hz, 1H, H-4$_\alpha$), 2.74 (m, 3H, H-1$_\beta$, H-2, H-4$_\beta$), 4.01 (q J = 6.6 Hz, 1H, H-12), 6.84 (s, 1H, H-8), 7,20 (s, 1H, H-5), 7.26−7.37 (m, 5H, Ph-ring) ppm; ^{13}C NMR (100 MHz, $CDCl_3$) δ = 22.2 (C-11), 25.0 (C-13), 27.1 (C-4), 28.6 (C-3), 35.8 (C-1), 50.3 (C-2), 50.3 (C-12), 121.7 (C-6), 128.5 (C-7), 131.4 (C-8), 132.0 (C-5), 134.7 (C-9), 135.7 (C-10), 126.5, 126.9, 128.5, 145.9 (Ph-ring) ppm; HRMS data were recorded using ESI positive ionization mode calcd for $C_{19}H_{23}BrN$ 344.1014; m/z M + 1, 344.1015.

23: ^{1}H NMR (600 MHz, $CDCl_3$) δ = 1.36 (d J = 6.6 Hz, 3H, H-13), 1.40 (br 1H, NH), 1.58 (m, 1H, H-3$_\beta$), 1.90 (m, 1H, H-3$_\alpha$), 2.27 (s, 3H, H-11), 2.57 (dd J^1 = 17.2 Hz, J^2 = 9.4 Hz, 2H, H-1$_\alpha$, H-4$_\alpha$), 2.74 (m, 2H, H-2, H-4$_\beta$), 2.97 (dd J^1 = 16.0 Hz, J^2 = 3.8 Hz, 1H, H-1$_\beta$), 4.00 (q J = 6.6 Hz, 1H, H-12), 6.77 (d J = 8.1 H-8), 7.29 (d J = 8.1 H-7), 7.26−7.37 (m, 5H, Ph-ring) ppm; ^{13}C NMR (100 MHz, $CDCl_3$) δ = 18.9 (C-11), 24.9 (C-13), 27.0 (C-4), 30.5 (C-3), 37.3 (C-1), 49.6 (C-2), 55.0 (C-12), 122.7 (C-6), 128.4 (C-8), 129.6 (C-7), 134.7 (C-5), 135.5 (C-10), 136.6 (C-9), 126.5, 127.0, 128.5, 145.4 (Ph-ring) ppm; HRMS data were recorded using ESI positive ionization mode calcd for $C_{19}H_{23}BrN$ 344.1014; m/z M + 1, 344.1014.

24: ^{1}H NMR (600 MHz, $CDCl_3$) δ = 1.33 (d J = 6.6 Hz, 3H, H-13), 1.40 (br 1H, NH), 1.54 (m, 1H, H-3$_\beta$), 2.08 (m, 1H, H-3$_\alpha$), 2.21 (s, 3H, H-11), 2.48 (m, 1H, H-1$_\alpha$), 2.51 (m, 1H, H-4$_\alpha$), 2.71 (m, 1H, H-2), 2.72 (m, 1H, H-1$_\beta$), 2.74 (m, 1H, H-4$_\beta$), 3.98 (q J = 6.6 H-12), 6.62 (d J = 8.4 H-8), 7.20 (d J = 8.4 H-7), 7.26−7.37 (m, 5H, Ph-ring) ppm; ^{13}C NMR (100 MHz, $CDCl_3$) δ = 19.0 (C-11), 24.6 (C-13), 26.8 (C-4), 29.7 (C-3), 36.6 (C-1), 49.8 (C-2), 55.0 (C-12), 122.7 (C-6), 128.2 (C-8), 129.8 (C-7), 134.6 (C-10), 135.5 (C-5), 136.4 (C-9), 126.5, 126.9, 128.5, 145.9 (Ph-ring) ppm; HRMS data were recorded using ESI positive ionization mode calcd for $C_{19}H_{23}BrN$ 344.1014; m/z M + 1, 344.1016.

■ ASSOCIATED CONTENT

Ⓢ Supporting Information

Proton and carbon NMR spectra of novel reported compounds **13**−**24** as well as the associated high-resolution mass spectra (HRMS). This material is available free of charge via the Internet at http://pubs.acs.org.

■ AUTHOR INFORMATION

Corresponding Author

*(H.-J.F.) Tel: +46 8 553 270 63. E-mail: hans-jurgen.federsel@astrazeneca.com. (W.T.) E-mail: wei.tian@astrazeneca.com.

Notes

The authors declare no competing financial interest.

■ ACKNOWLEDGMENTS

The skilled support provided by our AstraZeneca colleagues in the Analytical Science Department, Egil Forsberg, Margareta Andersson, and Dr Hefeng Pan, as well as Dr Susanne Olofsson in the Neuroscience Medicinal Chemistry unit, Södertälje, during the course of this investigation is gratefully acknowledged.

■ REFERENCES

(1) Stenfors, C.; Ahlgren, C.; Yu, H.; Wedén, M.; Larsson, L.-G.; Ross, S. B. *Psychopharmacology* **2004**, *172* (3), 333−340.

(2) Ahlgren, C.; Eriksson, A.; Tellefors, P.; Ross, S. B.; Stenfors, C.; Malmberg, Å. *Eur. J. Pharmacol.* **2004**, *499* (1−2), 67−75.

(3) Stenfors, C.; Hallerbäck, T.; Larsson, L.-G.; Wallsten, C.; Ross, S. B. *Naunyn-Schmiedeberg's Arch. Pharmacol.* **2004**, *369* (3), 330−337.

(4) Berg, S.; Linderberg, M.; Ross, S. B.; Thorberg, S.-O.; Ulff, B. PCT Int. Appl. WO 9,905,134, 1999.

(5) Federsel, H.-J.; Hedberg, M.; Qvarnström, F. R.; Sjögren, M. P. T.; Tian, W. *Acc. Chem. Res.* **2007**, *40* (12), 1377−1384.

(6) Federsel, H.-J.; Hedberg, M.; Qvarnström, F. R.; Tian, W. *Org. Process Res. Dev.* **2008**, *12* (3), 512−521.

(7) Sari, Y. *Neurosci. Biobehav. Rev.* **2004**, *28* (6), 565−582.

(8) (a) Vanhoenacker, G.; Dumont, E.; David, F.; Baker, A.; Sandra, P. *J. Chromatogr. A* **2009**, *1216* (16), 3563−3570. (b) Thyer, A. *Chem. Eng. News* **2010**, *88* (39), 16−26, 27−29. (c) Snodin, D. J. *Org. Process Res. Dev.* **2011**, *15* (6), 1243−1246.

(9) Rajšner, M.; Svátek, E.; Metyšová, J.; Bartošová, M.; Mikšik, F.; Protiva, M. *Collect. Czech. Chem. Commun.* **1977**, *42* (10), 3079−3093.

(10) Lewis, E. E.; Elderfield, R. C. *J. Org. Chem.* **1940**, *5* (3), 290−299.

(11) Burckhalter, J. H.; Campbell, J. R. *J. Org. Chem.* **1961**, *26* (11), 4232−4235. see also Rosowsky, A.; Battaglia, J.; Chen, K. K. N.; Modest, E. J. *J. Org. Chem.* **1968**, *33* (11), 4288−4290.

(12) Sims, J. J.; Cadogan, M.; Selman, L. H. *Tetrahedron Lett.* **1971**, *14*, 951−954.

(13) (a) Vaitiekunas, A.; Nord, F. F. *Nature* **1951**, *168* (4281), 875−876. (b) Vaitiekunas, A.; Nord, F. F. *J. Am. Chem. Soc.* **1953**, *75* (7), 1764−1768.

(14) Schnürch, M.; Spina, M.; Khan, A. F.; Mihovilovic, M. D.; Stanetty, P. *Chem. Soc. Rev.* **2007**, *36* (7), 1046−1057.
(15) Wotiz, J. H.; Huba, F. *J. Org. Chem.* **1959**, *24* (5), 595−598.
(16) Mach, M. H.; Bunnett, J. F. *J. Org. Chem.* **1980**, *45* (23), 4660−4666.
(17) (a) Olah, G. A.; Meyer, M. W. *J. Org. Chem.* **1962**, *27* (10), 3464−3469. (b) Olah, G. A.; LaPierre, J. C.; McDonald, G. J. *J. Org. Chem.* **1966**, *31* (4), 1262−1267.
(18) (a) Nordberg, P. Patent Appl. WO99/55706, 1999. (b) Miyano, S.; Fukushima, H.; Inagawa, H.; Hashimoto, H. *Bull. Chem. Soc. Jpn.* **1986**, *59* (10), 3285−3286. (c) Baker, R. W.; Foulkes, M. A.; Griggs, M.; Nguyen, B. N. *Tetrahedron Lett.* **2002**, *43* (51), 9319−9322.
(19) For a detailed description of the current procedure for benzylic bromination using NBS/$(BnO)_2$, see: *Organic Syntheses*; Wiley: New York, 1963; Collect. Vol. *IV*, pp 921−923.
(20) Pan, H.; Lundin, G. *Eur. J. Mass Spectrom.* **2011**, *17* (3), 217−225.